Materials and Structures/Matériaux et Constructions, Vol. 32, April 1999, pp 187-195

SCIENTIFIC REPORTS

Modelling cement microstructure: Pixels, particles, and property prediction

D. P. Bentz

Building and Fire Research Laboratory, National Institute of Standards and Technology, Gaithersburg, MD 20899 USA

Paper received: September 24, 1998; Paper accepted: October 26, 1998

ABSTRACT

During the past ten years, a comprehensive model for the three-dimensional microstructural development of cement paste during hydration has been developed and validated. The model employs a number of computational and analytical tools including cellular automata, digital image processing and reconstruction, percolation theory, and the maturity method. The model has been successfully applied to predicting the percolation and diffusion properties of cement pastes. Through a kinetics calibration, the evolution of heat release, chemical shrinkage, and compressive strength with time have been predicted. The variation of curing temperature and availability of external curing water can also be simulated using the developed model. This paper reviews the computational tools employed in the model, summarizes the experimental and modelling approaches, and presents representative predicted properties.

RÉSUMÉ

Durant les dix dernières années, un modèle tri-dimensionnel pour le développement microstructurel de la pâte de ciment pendant l'hydratation a été développé et validé. Le modèle utilise un certain nombre d'outils informatiques et analytiques incluant un automate cellulaire, l'analyse d'images numériques et la théorie de la percolation. Le modèle a été utilisé avec succès pour prédire les propriétés de percolation et de diffusion des pâtes de ciment. Grâce à un étalonnage cinétique, l'évolution du dégagement de chaleur, le retrait chimique et la résistance à la compression ont pu être prévus. La variation de température de maturation et la disponibilité de l'eau de cure externe, peuvent être également simulées en utilisant le modèle développé. Cet article passe en revue les outils informatiques utilisés dans le modèle, résume les approches expérimentales et de modélisation et présente les propriétés prévues par le modèle.

1. INTRODUCTION

As in all fields of science, materials science and civil engineering have benefited greatly from the evolution of computer hardware and software in the past few decades. Thus, it is no surprise that a new paradigm, computational materials science [1, 2], has been applied to the complex phenomena of cement hydration and microstructure development. Cement hydration is inherently complex [3]: a reaction system consisting of multi-size, multi-phase particles that evolves from a viscous suspension to a rigid load-bearing solid. However, this microstructure development needs to be better understood, because of its large influence on the transport and mechanical properties of these materials. Such an understanding could provide a major contribution to an integrated knowledge system for predicting concrete performance, such as the one currently being developed at the National Institute of Standards and Technology (NIST) under the auspices of the Partnership for High-Performance Concrete Technology program [4].

While the hydrated microstructure is easily observed in two dimensions using scanning electron microscopy (SEM), direct observation of the three-dimensional microstructure is extremely difficult. Since the percolation and other stereological properties of the three-dimensional structure greatly influence properties [5, 6], computer simulation of the three-dimensional microstructural development can provide critical knowledge on the relationships between microstructure and properties and lead to the design of improved materials. At NIST, a ten year research program has resulted in the development of a comprehensive computer model for the microstructural development of portland cement based systems [7]. The model is readily available to researchers for their use and further enhancement [8]. This paper

Editorial Note

Dr. D. P. Bentz is a RILEM Senior Member. He was awarded the Robert l'Hermite medal for 1998 for his outstanding achievements in the computer modelling of the formation and physical properties of cementitious materials. He presented a lecture of this paper at the 1998 RILEM Annual Meeting in Ballarat, Australia. He works at NIST (USA), a RILEM Titular Member.

1359-5997/99

briefly describes the computational tools employed in the model and presents a summary of experimental and computer model results obtained to date.

2. COMPUTATIONAL TOOLS

2.1 Digital images

The application of digital image processing [9] to problems in materials science and civil engineering has grown rapidly in recent years as witnessed by the emergence of conferences totally devoted to this topic [10]. While often applied at the structural level, analysis of digital images of cement-based materials at the micrometer level has provided a quantitative characterization tool for starting materials [11, 12] and hydrated systems [13]. A digital image typically consists of a two-dimensional array of pixels, each assigned a greylevel value (normally ranging from 0 to 255) indicative of the strength of a measured signal [9], such as reflected light intensity or the flux of backscattered electrons in an SEM image. Such images can be easily analyzed, using pixel counting for example, to determine quantities such as phase volume fractions and surface areas as well as the sizes and other stereological properties of individual particles. Figure 1 shows a digital image of a typical ASTM Type I ordinary portland cement (OPC) [14], obtained using an SEM, in which the component clinker phases have been identified [15].

Although difficult to obtain experimentally, computationally, this concept can be easily extended to three dimensions. In our simulations, each pixel occupies a finite volume, typically 1 μm^3, and is assigned to a specific mineralogical phase or porosity. In two or three dimensions, these digital images are easily mapped onto finite difference or finite element grids for the subsequent computation of properties such as electrical conductivity or elastic modulus [16]. Typically, these images are generated and analyzed in a static manner. It is, however, the ability to make dynamic modifications of such starting images through computational modelling that offers great potential for the simulation of microstructure development during hydration.

2.2 Cellular automata

When considering computational models of microstructure, a classification can be made into continuum models and discrete or digital-image-based models [5]. Continuum models consider the microstructure as a set of particles, typically spheres, and simulate microstructural development by modifying the particle attributes such as radius [17]. Digital-image-based models consider these materials at the sub-particle level and operate on all of the pixels comprising the microstructure using a series of cellular automaton (CA) rules. A cellular automaton is basically a computer algorithm that is discrete in space and time and operates on a lattice of

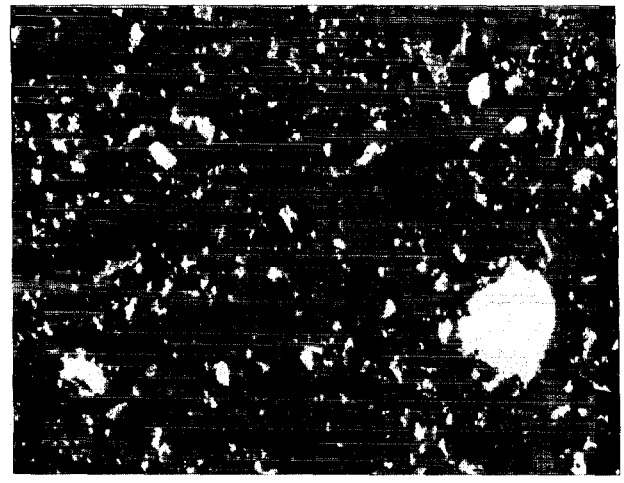

Fig. 1 – Final processed two-dimensional SEM/X-ray image of an OPC. Phases from brightest to darkest are: C_3A, gypsum, C_4AF, C_3S, C_2S, and porosity. Image is approximately 250 μm × 200 μm.

sites (in our case, pixels) [18, 19]. Examples of physical processes that can be simulated using CA-like rules include dissolution, precipitation, nucleation, and diffusion [7]. For example, to simulate random diffusion (Brownian motion), a diffusing species pixel may interchange its location with a neighboring porosity pixel chosen at random from all neighboring pixels. To simulate microstructural development over time, the CA rules are applied iteratively to all of the pixels comprising the microstructure. Thus, each cycle of the CA model corresponds to some unit of aging (curing) time in the physical material. After execution of each cycle of the model, digital image processing techniques may be employed to determine the new phase volume fractions, etc. In addition to the present model for cement hydration [5, 20], CA-type models have been developed for sintering [21], dendritic growth [22], and the carbonation of cement [23].

2.3 Percolation theory

Percolation theory considers the "connectedness" of a phase or multiple phases across a microstructure [24]. Formalized by Hammersley in the 1950's [25], it provides a technical basis for quantifying apparently random microstructures. Cement-based materials are essentially unique from a percolation standpoint, in that the percolation characteristics of several different phases influence properties [5, 6, 26, 27]: the commonly measured "set point" is a measure of the percolation of the solids in a hydrating cement paste system, the percolation/depercolation of the capillary porosity dominates the transport properties of these materials, and the percolation of calcium hydroxide can have a large influence on their durability [5, 28]. A common measure of percolation is the fraction of a phase that is part of a connected pathway across a microstructure. In a three-dimensional unit cube system, this would mean that portion of a phase which is connected (via a pathway totally remaining in

the phase) to two opposing faces of the microstructure. For digital images, this quantity can be easily assessed using a simple "burning algorithm" [24, 27]. An important item to note is that the percolation characteristics of a system are quite different in two and three dimensions. In three dimensions, a much smaller volume fraction of a phase (such as about 20%) can achieve percolation than in two dimensions (where 45% to 60% may be required).

2.4 Image reconstruction

Since for the prediction of performance, it is necessary to model the microstructural development of cement paste in three dimensions, realistic three-dimensional starting images of cement particles in water are needed. While SEM and X-ray imaging can provide segmented images of cement particles in two dimensions [15], such as that shown in Fig. 1, a direct three-dimensional measurement is impractical. Fortunately, three-dimensional image reconstruction techniques originally developed for two-phase porous materials [29-33] can be readily adapted to distribute the five cement phases (tricalcium silicate ($C_3S^{(1)}$), dicalcium silicate (C_2S), tricalcium aluminate (C_3A), tetracalcium aluminoferrite (C_4AF), and gypsum) amongst a collection of digitized spherical cement particles. It should be noted that the phases in an actual cement material are not limited to these five and that even these five do not typically exist in their pure form, but this simplification is commonly made for characterization and modelling purposes.

The image reconstructions rely on the fact that for an isotropic material, the autocorrelation function of a phase is the same in two and three dimensions. Thus, one can measure the autocorrelation functions in two dimensions for an actual image of the cement particles and employ them in a three-dimensional reconstruction. In the reconstructed three-dimensional image, the particle size distribution (PSD), phase volume fractions, and phase surface area fractions of the real cement powder can all be preserved [7].

2.5 Maturity method

In the real world, concrete is rarely produced under isothermal conditions. The maturity method has been developed to provide a quantitative technique for predicting the in-place compressive strength development of a concrete, based on its *in-situ* thermal history [34, 35]. The Arrhenius temperature dependence and time-temperature transformation used for compressive strength can also be applied to describing the degree of hydration as a function of time and temperature. In both cases, the dispersion models of Knudsen [36] can be employed to describe the time evolution of the property of interest. The parabolic form of this model takes the form:

$$A = A_u \frac{k\sqrt{(t-t_0)}}{1+k\sqrt{(t-t_0)}}$$

where A_u is the ultimate achievable value of the property, t_0 is an induction time, and k is a rate constant that typically follows an Arrhenius function with temperature. Assuming this functional form, model properties predicted in terms of number of cycles can be calibrated to experimental properties measured as a function of time. In addition, knowing the heats of reaction and heat capacities of the concrete materials [37], the adiabatic heat signature curve of a model concrete may be readily computed. This approach assumes that all of the cement reactions can be considered to have the same activation energy and underlying rate-controlling processes.

3. EXPERIMENTAL AND MODELLING APPROACH

The general procedure for modelling the behavior of a cement of interest is as follows. The cement to be modelled is potted in a low viscosity epoxy, the resin is cured, and the sample is polished and viewed in the SEM [15]. In addition to the backscattered electron image, a series of X-ray images are collected for a set of elements, typically, Ca, Si, Al, Fe, and S. This series of images is then processed to determine the mineralogical phase located at each pixel, resulting in a final image such as that shown in Fig. 1. For this two-dimensional image, the autocorrelation functions are measured for the following phase combinations: the silicates (tricalcium and dicalcium), the C_3S, and either the C_3A or the C_4AF, whichever is present in the greater volume fraction.

The next step in creating a starting three-dimensional image is to place digitized spherical particles at random locations in the three-dimensional computational volume following the measured PSD for the cement of interest such that the desired water-to-cement (w/c) ratio is obtained. Computationally, the particles are placed from largest to smallest to avoid the problem of not being able to find a location for a larger particle in a system already filled with much smaller ones. In this placement process, the particles can be placed totally at random, flocculated into a user-specified number of floc structures, or dispersed such that all cement particles are separated from one another by a specified distance (1 or 2 pixels). The flocculation and dispersion has major effects on the hydration needed to achieve set for model cement pastes [6], but has little influence on long term diffusion and percolation properties. During this placement process, a fraction of the particles are randomly assigned to be gypsum, with the remaining particles placed as cement, to be later assigned a specific mineralogical phase. Thus, the assumption is being made that the gypsum and cement follow the same PSD.

The final step in creating a realistic three-dimensional

(1) Conventional cement chemistry notation is used throughout this paper, C = CaO, S = SiO_2, A = Al_2O_3, F = Fe_2O_3, H = H_2O and $\bar{S}$ = SO_3.

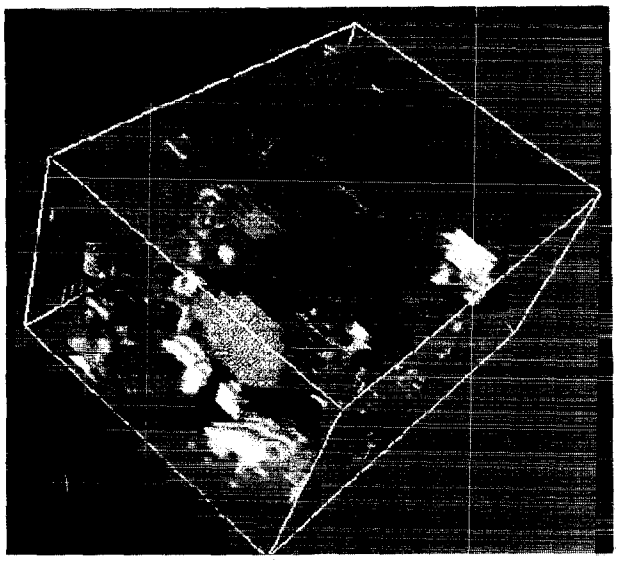

Fig. 2 – Portion of a reconstructed three-dimensional starting image for an OPC with w/c = 0.40. Aluminates are brightest, followed by gypsum, with silicates being the darkest grey and water-filled porosity black.

Table 1 – Physical properties of cementitious materials

Compound Name	Compound formula	Density (Mg/m^3)	Molar volume (cm^3/mole)	Heat of form. (kJ/mole)
Tricalcium silicate	C_3S	3.21	71.	-2927.82
Dicalcium silicate	C_2S	3.28	52.	-2311.6
Tricalcium aluminate	C_3A	3.03	89.1	-3587.8
Tetracalcium aluminoferrite	C_4AF	3.73	128	-5090.3
Gypsum	$C\bar{S}H_2$	2.32	74.2	-2022.6
Calcium silicate hydrate, C-S-H	$C_{1.7}SH_4$	2.12	108	-3283.
Calcium hydroxide	CH	2.24	33.1	-986.1
Ettringite	$C_6A\bar{S}_3H_{32}$	1.7	735.	-17539.
Monosulfate	$C_4A\bar{S}H_{12}$	1.99	313.	-8778.
Hydrogarnet	C_3AH_6	2.52	150.	-5548.
Iron hydroxide	FH_3	3.0	69.8	-823.9
Water	H	1.0	18.0	-285.83

image of the cement particles is to distribute the cement clinker phases amongst the particles assigned to be cement during particle placement [8]. The measured autocorrelation functions are used to create a three-dimensional filter that is applied to an image of Gaussian random noise overlaid on the 3-D cement particle image. After the filtering process, the correlated random noise image is thresholded to obtain the requested volume fraction of a specific phase. A curvature assessment algorithm [21] is then employed to match the surface area fraction of the phase to that measured in the real 2-D image. This procedure is first executed to separate the cement into silicates and aluminates. In two further executions of the programs, the silicates are further separated into C_3S and C_2S, and the aluminates into C_3A and C_4AF, resulting in a final 3-D image that is ready to be submitted to the hydration model. A portion of such an image for a typical OPC is given in Fig. 2.

The hydration model implements a series of CA rules to simulate the reactions that occur between the starting cement phases and water [7, 38]. To accurately simulate these reactions, the densities, molar volumes, and heats of formation of the individual compounds are required. Table 1 summarizes the values employed for these parameters in the current version of the microstructure model [39]. Using these values, each hydration reaction can be expressed in terms of volumetric units (pixels) for implementation in the model. Because in many cases, the volume occupied by the hydration products is less than that of the reactants, empty pore space may be created within the model 3-D structure to simulate the process of chemical shrinkage and self-desiccation [40], which can have a major influence on kinetics and properties in low w/c ratio systems.

To calibrate the kinetics of the model, a detailed set of experiments was conducted for two OPCs at each of three different w/c ratios and three different temperatures (15°C, 25°C, and 35°C) [7]. The experimental and modelling program for this validation exercise is outlined in Fig. 3. The two cements were characterized by SEM and PSD analysis to provide the needed model inputs. Experimentally, degree of hydration was quantified in three different fashions: non-evaporable water, heat release, and chemical shrinkage. Excellent correlation was observed between these three measures of the hydration progress [7]. Once the model was calibrated for one of the cements at one w/c ratio, it was able to successfully predict these properties for both of the cements at the three different w/c ratios, as well as the effects of curing under sealed as opposed to saturated conditions.

4. RESULTS

4.1 Percolation

As mentioned above, hydrating cement paste is a material rich in percolation phenomena. The microstructure model can provide quantitative information on the evolution of these percolation processes during hydration. Figure 4 shows this evolution with degree of hydration for the two major percolation processes of interest: percolation of total solids (set and strength development) and depercolation of capillary porosity (transport properties). In this case, an initial starting microstructure for a typical OPC was created with a w/c = 0.4 and all of the cement particles flocculated into a single floc structure, simulating the absence of any sort of dispersing agent (water reducer or superplasticizer). For set, two cement particles are considered percolated only if they are connected by hydration prod-

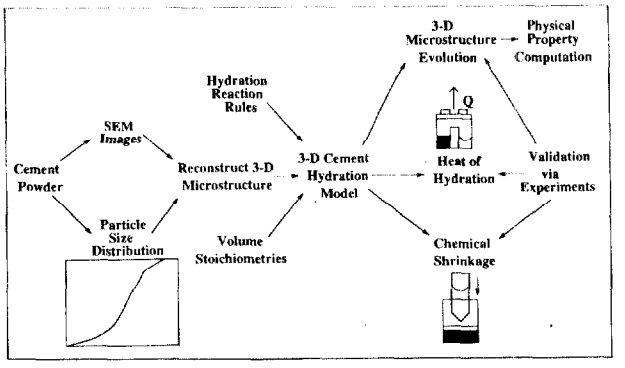

Fig. 3 – Flow diagram summarizing experimental and modelling program for predicting cement performance.

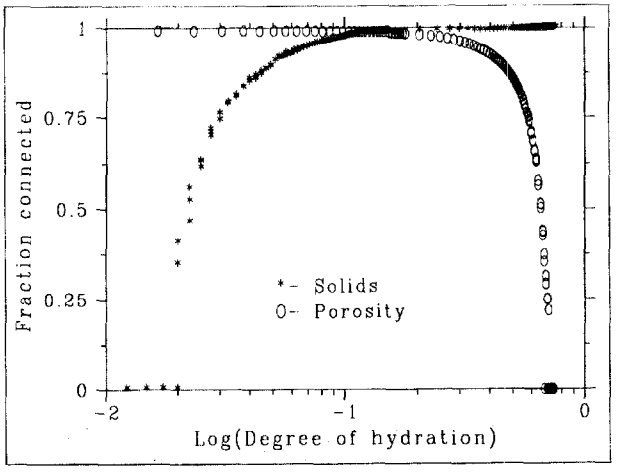

Fig. 4 – Percolation plots for an OPC paste (w/c = 0.4) showing fraction of phase connected for total solids and capillary porosity as a function of degree of hydration.

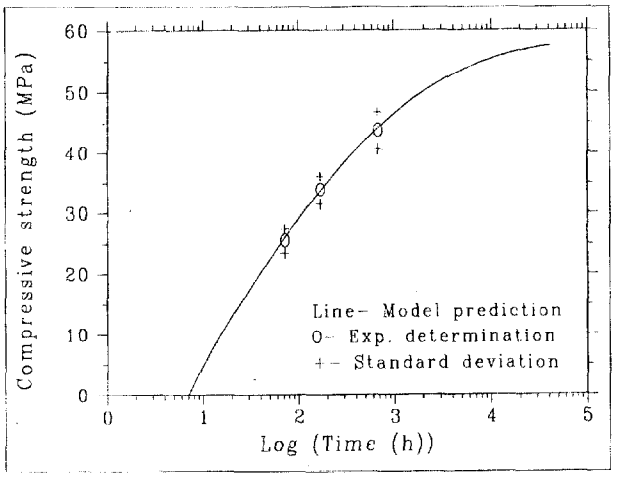

Fig. 5 – Model predicted and experimentally measured compressive strength development for an OPC paste. Crosses indicate standard deviation in experimentally measured values.

uct (calcium silicate hydrate gel (C-S-H) or ettringite) and not simply if they are touching (weaker bonding forces) [41]. For this flocculated system, only about 2% hydration is required to achieve set, in agreement with experimental measurements of shear resistance [42]. For a higher w/c value, 0.5, 3% hydration is needed to achieve set, as the cement particles are more separated at the higher initial w/c ratio.

The other key percolation aspect of hydrating cement pastes is the depercolation of the capillary porosity. In Fig. 4, one can see that the capillary porosity is highly connected throughout the early and middle stages of the hydration and then quickly loses connectivity and disconnects at about 70% hydration. This corresponds to a capillary porosity of about 21% in agreement with the values of 19-26% based on experimental measurements of permeability by Powers [43]. Previous results have shown that this percolation threshold on the order of 20% capillary porosity is independent of starting w/c ratio [27]. Thus, for a starting w/c ratio high enough such that, even at complete hydration, the capillary porosity exceeds 20% (*e.g.* w/c > 0.6) depercolation will never be achieved. Once the capillary porosity depercolates, transport processes will proceed at a much lower rate, as the primary pathway for transport will shift from the capillary pores to the much smaller gel pores present in the C-S-H. Based on these percolation results and direct simulations of the electrical conductivity of model cement pastes, an equation relating diffusivity to capillary porosity has been developed and validated for OPC pastes [44] and used in a multi-scale modelling approach to develop an equation that predicts the chloride ion diffusion coefficient of concrete as a function of mixture proportions [45].

4.2 Strength

The microstructure model can also be applied to predicting the compressive strength development of ASTM C109 mortar cubes [14]. To relate compressive strength to degree of hydration, the gel-space ratio concept originally developed by Powers and Brownyard is employed [46]. The gel-space ratio, X, is defined by [46]:

$$X = \frac{0.68\alpha}{0.32\alpha + \frac{w}{c}}$$

where α is the degree of hydration. It has been shown that the compressive strength of ASTM C109 mortar cubes, σ_c, can be related to the gel-space ratio *via*:

$$\sigma_c(t) = \sigma_A X(t)^n$$

where σ_A represents the intrinsic strength of the cement and n takes on values between 2.5 and 3. Since σ_A is typically not known *a priori*, a 3-day compressive strength measurement is used to obtain its value. Then, the microstructure model is executed and based on the evolution of hydration with time, the compressive strength vs. age is predicted, and compared to the values measured at 7 and 28 days. Figure 5 provides an example of the results obtained for a typical OPC [7]. The model is seen to accurately predict the measured development of strength with time well within the standard

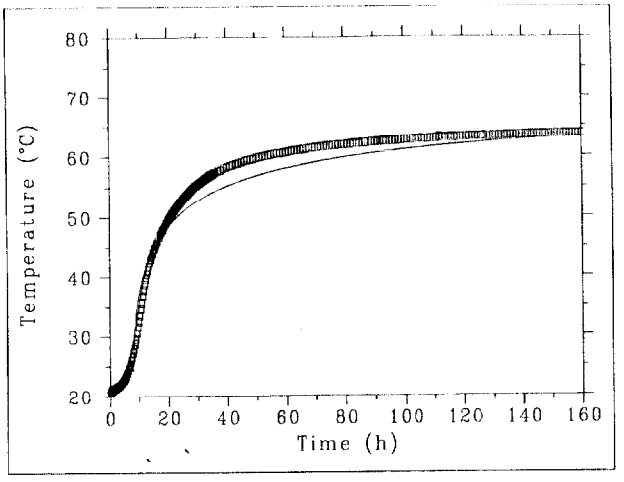

Fig. 6 – Comparison of experimental (data points) and simulated (solid line) adiabatic heat signature curves for a w/c = 0.65 OPC concrete.

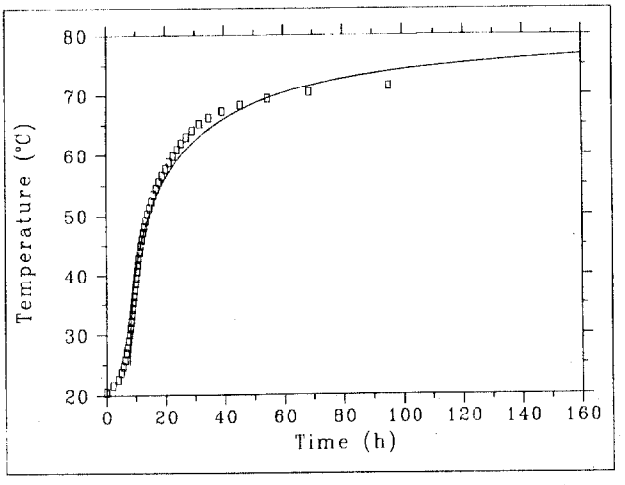

Fig. 7 – Comparison of experimental (data points) and simulated (solid line) adiabatic heat signature curves for a w/c = 0.65 OPC concrete with 10% by mass silica fume.

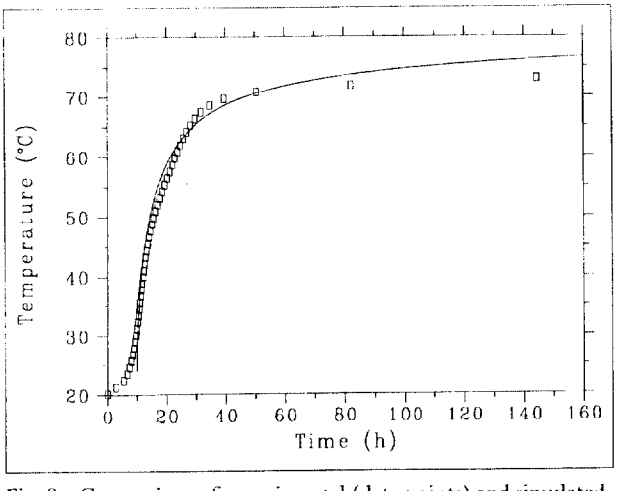

Fig. 8 – Comparison of experimental (data points) and simulated (solid line) adiabatic heat signature curves for a w/c = 0.65 OPC concrete with 50% by mass fly ash.

deviation of the experimental testing program, and could provide a means for reducing the standard 28 day testing to 3 days, with the possibility of confirmatory testing at 7 days.

4.3 Thermal history

A key concern for concrete in the field is thermal cracking at early ages [47, 48]. Because the cement hydration reactions are exothermic, large temperature gradients (on the order of 50°C) may be generated within a concrete structure. The microstructure model may be used to investigate the propensity for this phenomena by predicting the adiabatic heat signature curve for a specific concrete mix proportion [37]. Using a measured activation energy (typically on the order of 40 kJ/mol [7]), the Arrhenius function, and the maturity method, the temperature rise with time for a specimen hydrated under totally adiabatic conditions may be predicted [37]. Figures 6-8 provide a comparison of model and measured results for an OPC concrete, and the same system with silica fume [37] and fly ash [49]. For all three concretes, the model predictions are seen to lie within a few degrees Celsius of the experimental results. In both cases, the addition of pozzolanic materials is seen to significantly increase the temperature rise, causing the long term temperature of the concrete to exceed 70°C so that secondary ettringite formation may become a concern [3]. By coupling this model with a finite element model for a specific concrete structure, the propensity for thermal cracking under various curing regimes could be predicted.

4.4 Self-desiccation

In addition to temperature variation, another key environmental variable in the curing of concrete is the relative humidity or availability of curing water. Because the solid cement hydration products occupy less space than the starting solid reactants and water, external water will be imbibed into the concrete throughout its curing history. When external water is unavailable, empty porosity will be created within the cement paste, influencing reaction kinetics, microstructure, and physical properties. The NIST microstructure model can be operated under either saturated or sealed curing conditions [8]. Figure 9 provides a comparison of model and experimental results for degree of hydration vs. curing time for an OPC paste prepared with initial w/c = 0.30. The sealed curing conditions are seen to substantially hamper the progress of the hydration reactions at longer times (> 7 days). The agreement between the model predictions and experimental measurements is observed to be well within the scatter of the experimental data.

The microstructure model also allows a direct observation of the resulting microstructure for hydration performed under saturated and sealed conditions. Figure 10 provides a set of two-dimensional images from the final

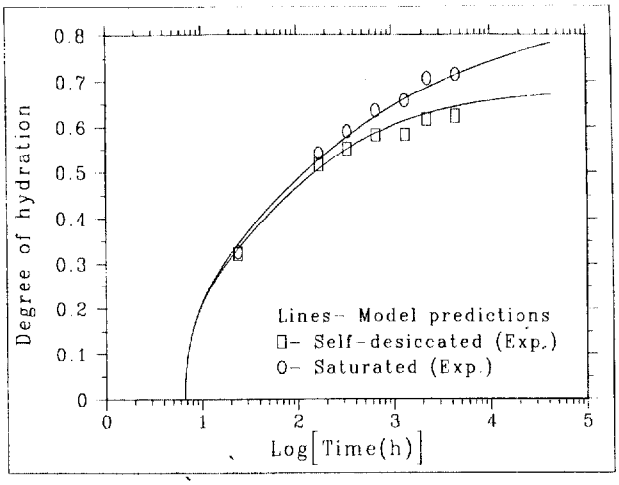

Fig. 9 – Comparison of model predicted (solid lines) and measured (data points) degree of hydration for a w/c = 0.30 OPC paste hydrated under saturated and sealed curing conditions at 25°C.

three-dimensional simulated microstructures for a w/c = 0.30 OPC paste hydrated under the two different curing conditions, as well as two real SEM images obtained on the experimental counterparts of the model systems [40]. The effects of self-desiccation are clearly evident as the microstructure formed under sealed curing contains many large capillary pores and large grains of unhydrated cement, both of which are practically eliminated under saturated curing. The increased volume of unhydrated cement present under sealed curing is consistent with the degree of hydration results presented in Fig. 9. The model microstructural images are seen to compare very favorably with their equivalent SEM counterparts obtained directly on the real hydrated cement pastes.

While the empty porosity created during sealed curing definitely leads to a lower compressive strength, its effects on transport properties are not well determined. If the pores remain empty, they provide no pathway for transport, effectively acting as inert filler material. However, if these pores later refill with water, without any accompanying increase in the formation of hydration products (a worst case scenario), the effects on transport properties could be dramatic. By directly computing the relative electrical conductivity (equivalent to the relative diffusivity [44]) using a conjugate gradient technique [16], these effects can be quantified. Figure 11 provides a comparison of model results for a w/c = 0.4 OPC paste. In both cases, the diffusivity is seen to decrease with increasing degree of hydration in a characteristic S-shaped manner [44]. However, because of the rather large volume fraction of empty capillary porosity present in the microstructures at later ages, resaturation may increase the diffusivity of these materials by up to a factor of three or more. Since, for many degradation processes, service life is directly proportional to a diffusion coefficient [50], this could result in a threefold

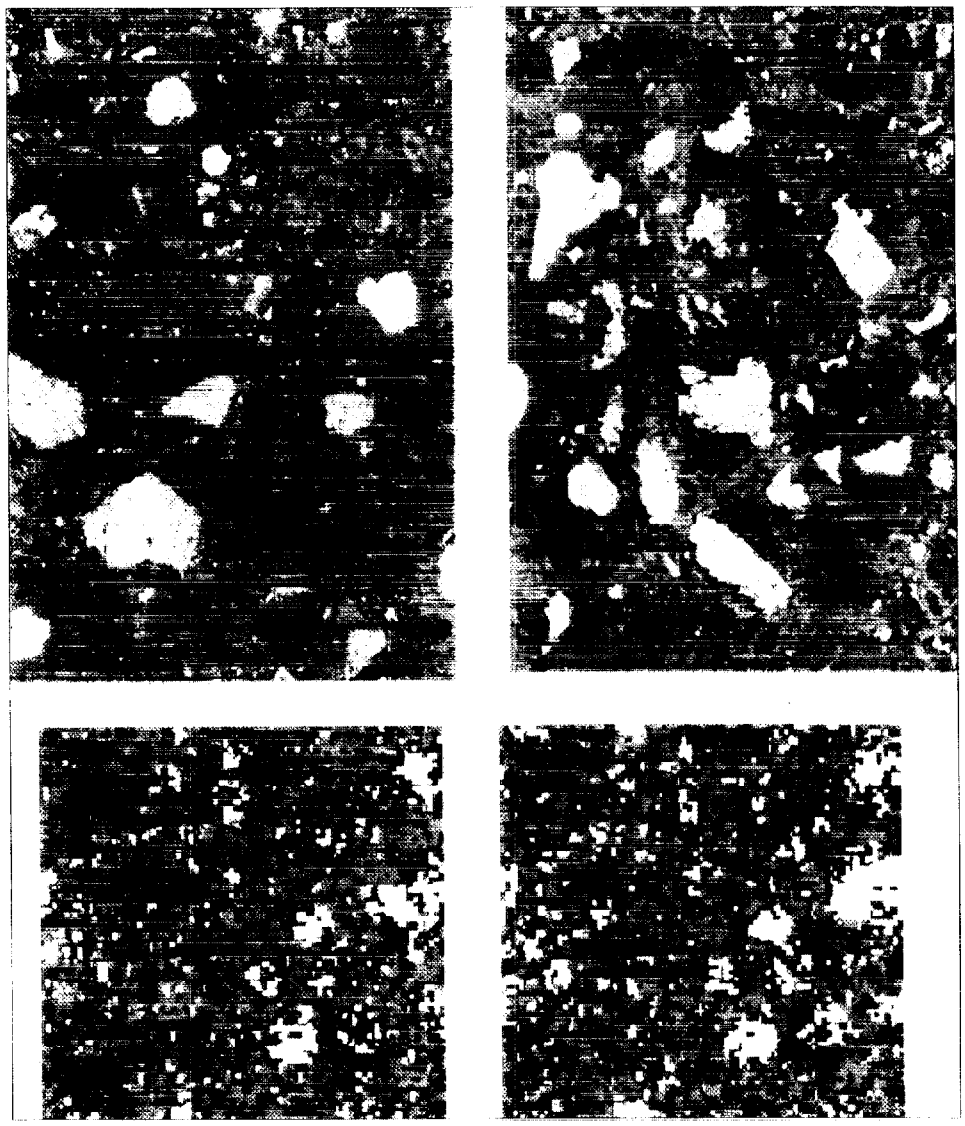

Fig. 10 – Comparison of two-dimensional images from real and microstructure model cement pastes for a w/c = 0.30 OPC paste hydrated under saturated (left) and sealed (right) curing conditions. Black is capillary porosity and white is unhydrated cement. Light grey is calcium hydroxide and dark grey is C-S-H gel and other hydration products. Real images are 128 μm × 190 μm. Model images are 100 μm × 100 μm.

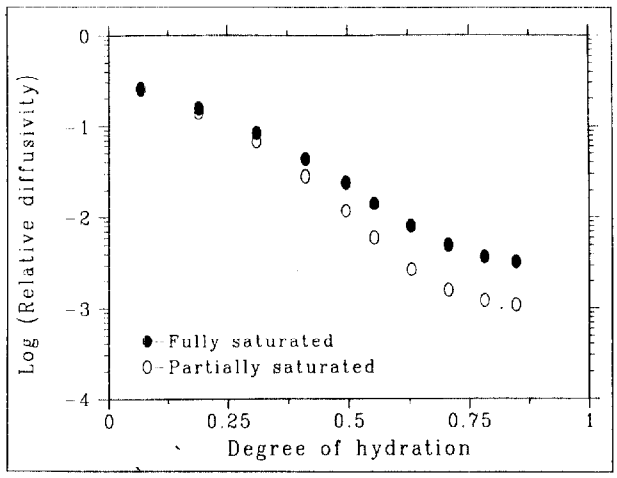

Fig. 11 – Relative diffusivity vs. degree of hydration for a w/c = 0.4 OPC paste hydrated under sealed curing conditions. Filled circles indicate case where all pores are resaturated with water while hollow circles indicate original partially saturated systems.

reduction in usable life for a concrete structure. Thus, understanding both the microstructure and environmental exposure of these materials is critical in the design and rehabilitation of concrete structures.

5. CONCLUSIONS

A variety of applications of a three-dimensional digital-image-based computer model to studying cement hydration and properties has been demonstrated. The model provides a deeper understanding of the effects of physical microstructure and environmental variables on properties. As new and more detailed information becomes available on the basic mechanisms of cement hydration, the model will be concurrently updated to remove some of the assumptions currently being employed. As the model continues to be developed, it will provide a basis for examining new cement-based materials and optimizing formulations for a specific desired set of physical properties. Current research is focused on extending the model to incorporate pozzolanic materials; the incorporation of silica fume has been successfully completed [37] and that of fly ash is currently in progress [49]. Longer term efforts will focus on allowing compositional and molar volume variations in the C-S-H gel and incorporating an induction period mechanism into the model so that the very early time behavior of these complex materials may be better simulated.

ACKNOWLEDGEMENTS

The author would like to thank his many colleagues in the Building Materials Division at NIST who have contributed to this research, especially Dr. Edward Garboczi, who was instrumental in the early stages of the model development and the application of percolation theory to these materials. He would also like to thank V. Waller and F. de Larrard of Laboratoire Central des Ponts et Chaussées, France for providing the experimental adiabatic heat signature data used in Figs. 6-8 and Paul Stutzman of NIST for obtaining the real SEM images presented in Fig. 10.

REFERENCES

[1] Garboczi, E. J. and Bentz, D. P., 'Computational materials science of cement-based materials', *MRS Bull.* **28** (3) (1993) 50-54.

[2] Garboczi, E. J. and Bentz, D. P., 'Computational materials science on the internet', *ACI Concr. Internat.* **19** (12) (1998) 26-27, see also the monograph available over the Internet at http://ciks.cbt.nist.gov/garbocz/.

[3] Taylor, H. F. W., 'Cement Chemistry', 2nd. Edn. (Thomas Telford, London, 1997).

[4] Frohnsdorff, G., 'Partnership for high-performance concrete', in 'Proceedings of the International Symposium on High-Performance and Reactive Powder Concretes', Ed. P.C. Aitcin, (1998) 51-73.

[5] Bentz, D. P. and Garboczi, E. J., 'Modelling the leaching of calcium hydroxide from cement paste: Effects on pore space percolation and diffusivity', *Mater. Struct.* **25** (1992) 523-533.

[6] Bentz, D. P., Garboczi, E. J. and Martys, N. S., 'Application of digital-image-based models to microstructure, transport properties, and degradation of cement-based materials', in 'The Modelling of Microstructure and Its Potential for Studying Transport Properties and Durability', Ed. H. M. Jennings, J. Kropp, and K. L. Scrivener (Kluwer Academic Publishers, Dordrecht, 1996) 167-185.

[7] Bentz, D. P., 'Three-dimensional computer simulation of portland cement hydration and microstructure development', *J. Am. Ceram. Soc.* **80** (1) (1997) 3-21.

[8] Bentz, D. P., 'Guide to using CEMHYD3D: A three-dimensional cement hydration and microstructure development modelling package', NISTIR 5977, U.S. Dept. of Commerce, February 1997, software and manual available over the Internet from anonymous ftp at edsel.cbt.nist.gov (129.6.104.138) in the /pub/CEMHYD3D subdirectory.

[9] Castleman, K. R., 'Digital Image Processing', (Prentice-Hall, Inc., Englewood Cliffs, NJ, 1979).

[10] 'Digital Image Processing: Techniques and Applications in Civil Engineering', Ed. J. D. Frost and J. R. Wright (American Society of Civil Engineers, 1993).

[11] Scrivener, K. L., 'The microstructure of anhydrous cement and its effect on hydration', in Proceedings, Materials Research Society Symposia, 85, Ed. L. J. Struble and P. W. Brown (Materials Research Society, Pittsburgh, PA, 1987) 39-46.

[12] Stutzman, P. E., 'Cement clinker characterization by scanning electron microscopy', *Cem. Concr. Aggregates* **13** (2) (1991) 109-114.

[13] Scrivener, K. L., and Pratt, P. L., 'Characterization of interfacial microstructure', in 'Interfacial Transition Zone in Concrete', Ed. J. C. Maso (E & FN Spon, London, 1996) 3-17.

[14] 'Annual Book of ASTM Standards', Vol. 04.01. Cement; Lime; Gypsum (ASTM, Philadelphia, PA, 1995).

[15] Bentz, D. P. and Stutzman, P. E., 'SEM analysis and computer modelling of hydration of portland cement particles', in 'Petrography of Cementitious Materials', Ed. S. M. DeHayes and D. Stark (ASTM, Philadelphia, PA, 1994) 60-73.

[16] Garboczi, E. J., 'Manual for finite difference and finite element techniques', NISTIR 6269 U.S. Dept. of Commerce, Dec. 1998, also available over the Internet at http://ciks.cbt.nist.gov/garbocz/.

[17] Jennings, H. M. and Johnson, S. K., 'Simulation of microstructure development during the hydration of a cement compound', *J. Am. Ceram. Soc.* **69** (1986) 790-795.

[18] 'Cellular Automata: Theory and Experiment', Ed. J. Gutowitz (MIT Press, Cambridge, MA, 1991).

[19] Wolfram, S., 'Theory and Applications of Cellular Automata', (World Scientific, Singapore, 1986).

[20] Bentz, D. P., Coveney, P., Garboczi, E. J., Kleyn, M. and

Stutzman, P. E., 'Cellular automaton simulations of cement hydration and microstructure development', *Modell. Simul. Mater. Sci. Eng.* **2** (4) (1994) 783-808.
[21] Pimienta, P. J., Garboczi, E. J. and Carter, W. C., 'Cellular automaton algorithm for surface mass transport due to curvature gradients: Simulations of sintering', *Comput. Mater. Sci.* **1** (1992) 63-77.
[22] Spittle, J. A. and Brown, S. G. R., 'A cellular automaton model of steady-state columnar-dendritic growth in binary alloys', *J. Mater. Sci.* **30** (1995) 3989-3994.
[23] Karapiperis, T., 'Cellular automaton model of precipitation/dissolution coupled with solute transport', *J. Stat. Phys.* **81** (1995) 165-180.
[24] Stauffer, D. and Aharony, A., 'Introduction to Percolation Theory', 2nd. Edn. (Taylor and Francis, London, 1992).
[25] Hammersley, J. M., *Proc. Cambridge Phil. Soc.* **53** (1957) 642.
[26] Garboczi, E. J. and Bentz, D. P., 'The microstructure of portland cement-based materials: Computer simulation and percolation theory', *Mat. Res. Soc. Symp. Proc.*, **Vol. 529** (1998) 89-100.
[27] Bentz, D. P. and Garboczi, E. J., 'Percolation of phases in a three-dimensional cement paste microstructure model', *Cem. Concr. Res.* **21** (2/3) (1991) 325-344.
[28] van Eijk, R. J. and Brouwers, H. J. H., 'Study of the relation between hydrated portland cement composition and leaching resistance', *Ibid.* **28** (6) (1998) 815-828.
[29] Joshi, M., 'A Class of Stochastic Models for Porous Media', Ph. D. Thesis, Univ. of Kansas, 1974.
[30] Quiblier, J. A., 'A new three-dimensional modeling technique for studying porous media', *J. Colloid. Inter. Sci.* **98** (1) (1984) 84-102.
[31] Bentz, D. P. and Martys, N. S., 'Hydraulic radius and transport in reconstructed model three-dimensional porous media', *Transport in Porous Media* **17** (3) (1994) 221-238.
[32] Quenard, D. A., Xu, K., Kunzel, H. M., Bentz, D. P. and Martys, N. S., 'Microstructure and transport properties of porous building materials', *Mater. Struct.* **31** (209) (1998) 317-324.
[33] Bentz, D. P., Garboczi, E. J. and Quenard, D. A., 'Modelling drying shrinkage in reconstructed porous materials: Application to porous vycor glass', *Modell. Simul. Mater. Sci. Eng.* **6** (1998) 1-26.
[34] Carino, N. J., 'The maturity method: Theory and application', *Cem. Concr. Aggregates* **6** (2) (1984) 61-73.
[35] Carino, N. J., Knab, L. I. and Clifton, J. R., 'Applicability of the Maturity Method to High-Performance Concrete', NISTIR 4819, U.S. Dept. of Commerce, May 1992.
[36] Knudsen, T., 'The dispersion model for hydration of portland cement I. general concepts', *Cem. Concr. Res.* **14** (1984) 622-630.
[37] Bentz, D. P., Waller, V. and de Larrard, F., 'Prediction of the adiabatic temperature rise in conventional and high-performance concretes using a 3-D microstructure model', *Ibid.* **28** (2) (1998) 285-297.
[38] RILEM Technical Committee 66-MMH, 'Mathematical modelling of hydration of cement: The hydration of tricalcium aluminate and tetracalcium aluminoferrite in the presence of calcium sulfate', *Mater. Struct.* **19** (1986) 137-.
[39] 'Handbook of Chemistry and Physics', 63rd Edn., (CRC Press, Boca Raton, FL, 1982) B73-B166 and D52-D95.
[40] Bentz, D. P., Snyder, K. A. and Stutzman, P. E., 'Microstructure modelling of self-desiccation during hydration', in 'Self-Desiccation and Its Importance in Concrete Technology', Ed. B. Persson and G. Fagerlund (Lund Institute of Technology, Lund, Sweden, 1997) 132-140.
[41] Nonat, A., 'Interactions between chemical evolution (hydration) and physical evolution (setting) in the case of tricalcium silicate', *Mater. Struct.* **27** (1994) 187-195.
[42] Jiang, S. P., Mutin, J. C. and Nonat, A., 'Studies on mechanism and physico-chemical parameters at the origin of cement setting: I. the fundamental processes involved during the cement setting', *Cem. Concr. Res.* **24** (4) (1995) 779-789.
[43] Powers, T. C., Copeland, L. E., and Mann, H. M., *PCA Bulletin* **10** (1959).
[44] Garboczi, E. J. and Bentz, D. P., 'Computer simulation of the diffusivity of cement-based materials', *J. Mater. Sci.* **27** (1992) 2083-2092.
[45] Bentz, D. P., Garboczi, E. J. and Lagergren, E. S., 'Multi-scale microstructure modeling of concrete diffusivity: Identification of significant variables', *Cem. Concr. Aggregates* **20** (1) (1998) 129-139.
[46] Mindess, S. and Young, J. F., 'Concrete', (Prentice-Hall, Englewood Cliffs, NJ, 1981).
[47] Waller, V., de Larrard, F. and Roussel, P., 4th Int. Symp. Utilization of High-Strength/High-Performance Concrete, RILEM (1996) 415-421.
[48] 'Thermal Cracking in Concrete at Early Ages', (E & FN Spon, London, 1995).
[49] Bentz, D. P. and Remond, S., 'Incorporation of Fly Ash into a 3-D Cement Hydration Microstructure Model', NISTIR 6050, U.S. Dept. of Commerce, August 1997.
[50] Clifton, J. R. and Knab, L. I., 'Service Life of Concrete', NISTIR 89-4086, U.S. Dept. of Commerce, 1989.